Detection of the Earth's rotation using superfluid phase coherence

Keith Schwab, Niels Bruckner & Richard E. Packard

Physics Department, University of California, Berkeley, California 94707, USA

It has long been recognized that the macroscopic quantum properties of superfluid helium could form the basis of a technique for measuring the state of absolute rotation of the containment vessel[1–5]: circulation of superfluid helium is quantized, so providing a reference state of zero rotation with respect to inertial space. Here we provide experimental proof of this concept by detecting the rotation of the Earth using the spatial phase coherence of superfluid ^{4}He, thus providing independent corroboration of an earlier report[6] that demonstrated the feasibility of making such a measurement. Our superfluid container is constructed on a centimetre-size silicon wafer, and has an essentially toroidal geometry but with the flow path interrupted by partition incorporating a sub-micrometre aperture. Rotation of the container induces a measurable flow velocity through the aperture in order to maintain coherence in the quantum phase of the superfluid. Using this device, we determine the Earth's rotation rate to a precision of 0.5% with a measurement time of one hour, and argue that improvements in sensitivity of several orders of magnitude should be feasible.

The idea at the foundation of the experiment is that the superfluid state is described by a macroscopic quantum phase, ϕ, whose gradient is proportional to the superfluid velocity. This leads to the conclusion that, if the wavefunction is single-valued, the integral of the velocity around a closed curve (that is, the circulation) must be quantized:

$$\oint v_s \mathrm{d}l = \frac{h}{2\pi m}\oint \nabla\phi \mathrm{d}l = n\frac{h}{m} \qquad n = 0, 1, 2, \ldots \qquad (1)$$

Here, h is Planck's constant and m is the atomic mass of ^{4}He.

In a container rotating at small angular velocity, the ground state of the superfluid has zero circulation. If the container is not symmetric with respect to the rotation axis, the superfluid must move to avoid the moving boundaries, but the induced flow must always satisfy equation (1).

We now consider a toroidal container of average radius R, interrupted by a septum which is pierced by a submicrometre aperture (Fig. 1a); the torus is slowly rotating at angular velocity ω. The moving septum induces the fluid in the body of the torus to flow, almost like a solid body ($v_s = \omega R$). To satisfy equation (1), when the circulation integral traverses the torus and passes through the aperture, there must be an induced velocity v_s in the aperture, that cancels the solid-body flow contributions from the bulk of the torus. The rotation-induced velocity in the aperture is given by

$$v_a = \frac{2\omega\pi R^2}{l_{\mathrm{eff}}}\cos\theta \qquad (2)$$

where R is the radius of the torus and l_{eff} is an effective length of the aperture. The $\cos\theta$ factor accounts for the general case when the axis of rotation is inclined at an angle θ with respect to the normal to the toroidal plane.

Our experiment consists of measuring the rotation-induced velocity with apparatus which is a superfluid analogue of a superconducting a.c. SQUID[7,8].

The device, shown in Fig. 1b, is a Helmholtz oscillator similar to that used to detect single phase slips[9]. A description of the device is given in the figure legend. The tension of the membrane that seals the upper surface of the device provides the potential energy reservoir, and the fluid passing through the central microaperture and around the peripheral channel provides the kinetic-energy reservoir. The oscillator has a resonant frequency of 66 Hz and exhibits a Q of 20,000 at $T = 280$ mK, the typical operating temperature.

Figure 2 is a plot of the oscillation amplitude as a function of the applied electric drive. The observed staircase pattern is a characteristic feature of these double-hole devices[10]. The plateau represented by the first step is due to the fluid reaching the intrinsic critical velocity for quantized vortex creation in the aperture. When a vortex is created in the hole, it passes across the aperture removing a discrete amount of energy from the flow. The quantum phase

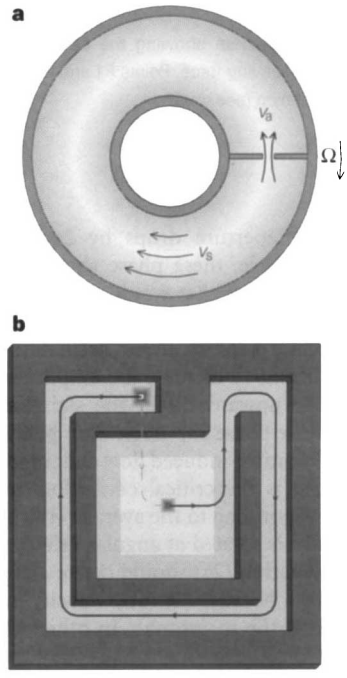

Figure 1 a, A torus rotating at angular velocity Ω, partitioned by a septum containing a small aperture. Backflow through the aperture, at velocity v_a, is induced by the rotation to keep the circulation equal to zero. The superfluid velocity v_s approximates that of a solid body. **b**, The superfluid rotation sensor built on a silicon wafer[11]. A central square depression continues around the periphery of the chip and terminates near a relatively large window (1 mm square) opening to the back of the wafer. The depressed areas (80 μm deep) are covered and sealed with an 8-μm-thick Kapton diaphragm epoxied to the raised silicon surface. A single small aperture[12] (190 nm × 1,000 nm in a 100-nm-thick silicon nitride wall), also opening to the back of the wafer, is placed in the centre of the central square depression. The device is placed in a superfluid-filled enclosure. There is a continuous path within the fluid: from the top surface of the microaperture, around the peripheral channel, through the large hole to the back of the wafer, and through the microaperture back into the central depression. This path serves as the toroidal geometry mentioned above. The mean length, L, of each side of the channel is 10.5 mm and the channel width is 1.5 mm. If the device is rotated, the induced velocity in the aperture is given by equation (2) with the effective area (πR^2 in equation (2)) equal to $0.93L^2$. The arrowed line indicates a path of integration for the circulation. The solid segment lies within the etched channels and the dotted line represents a path on the back surface of the wafer. The Kapton membrane is metallized on both sides, and can be moved by applying an electric potential to an electrode positioned in the central depression. The membrane's resultant position is monitored with a superconducting displacement transducer[13] having a resolution of 10^{-15} m Hz$^{-1/2}$.

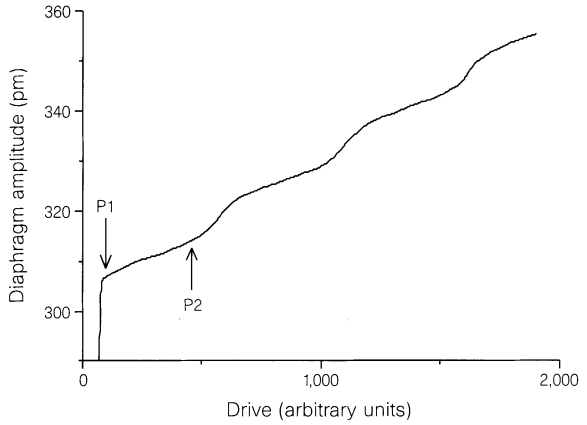

Figure 2 The staircase response showing the oscillation amplitude of the diaphragm as a function of driving force. Points P1 and P2 are two typical points monitored during reorientation (see text).

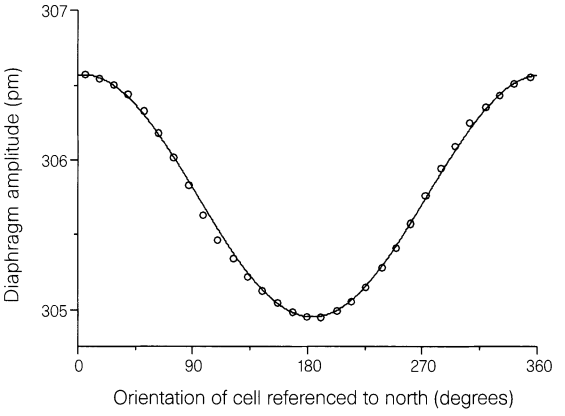

Figure 3 The oscillation amplitude at point P1 (in Fig. 2) as a function of orientation of the chip with respect to north. The oscillation amplitude is smoothed by a lock-in amplifier with a time constant of 10 s. The data (circles), which are digitally recorded at 0.5 points per s, is then averaged with a sliding average using 250 points. Point P2 shows a similar modulation but is out of phase by π. The solid curve is a fit of the data to a cosine function.

difference across the aperture drops by 2π. As the oscillator proceeds through its cycle, these phase slips occur in pairs and limit the amplitude increase that would otherwise accompany an increasing drive level. Subsequent steps are produced when, after an even number of phase slips in every oscillation half-cycle, the driving force is sufficient to increase the amplitude until addition slip pairs occur. The upward tilt in the staircase is due to the stochastic nature of the phase slip nucleation process[9].

In the absence of rotation-induced flow and trapped vorticity, the level of the first step is the critical oscillation amplitude of the membrane, A_c, corresponding to the average critical velocity in the aperture. If the device is rotated at angular velocity ω, the induced velocity (given by equation (2)) should create an apparent shift in the level of the plateau because the total velocity in the aperture is not directly sensed by the membrane. In other words, the membrane motion is responsible for only a fraction of the actual velocity in the aperture. The remaining fraction includes the rotation-induced flow plus residual bias flow from trapped vorticity. Thus the oscillation amplitude on the nth plateau A_n is given by

$$A_n = A_c - B\omega + C \qquad (3)$$

where B is a known geometric factor involving the areas of the membrane and the aperture and C represents the effect of bias currents. On a given plateau, A_n is bounded between levels corresponding to 0 and π phase difference across the aperture. Therefore an unbounded increase in ω would result in a triangle response in A_n.

The normal to the plane of our torus (a silicon wafer) lies in a horizontal plane. The device can be reoriented with respect to the compass by rotating the entire crysostat about a vertical axis. If one monitors the level on a given point of a plateau, we expect the level to shift with rotation flux. Our sensor has sufficient loop area that the rotation of the Earth at our latitude (38° N) corresponds to a maximum phase shift of $\sim \pm \pi/4$. If the normal to the plane of the torus points in an east–west direction, the Earth's rotation creates no flux through the loop. If the normal is oriented at angle α with respect to a meridian, the Earth's rotation flux through the loop is $2\omega\pi R^2 \cos 38° \cos\alpha$. Thus when the apparatus is reoriented around a vertical axis we expect a $\cos\alpha$ dependence of the amplitude of point P1 on the first plateau in Fig. 2. Other points along the staircase are expected to be modulated with α in a periodic manner, possibly offset and inverted. The expected modulation pattern depends on the value of any fixed bias phase difference that might exist across the aperture. These phase biases may arise from vortex lines pinned anywhere in the flow path. The motion of a single vortex across the peripheral channel causes a 2π shift across the aperture. Therefore the successful operation of the rotation sensor depends on there being no vortex motion during the course of a measurement. In practice this is difficult to achieve. The data must be recorded at night, when mechanical noise arising from human activity in the building is at a minimum.

Figure 3 shows the measured correlation between point P1 (Fig. 2) on the first plateau level and the orientation angle of the torus, α. To record this data the entire cryostat is smoothly rotated at about one revolution per hour.

The solid line drawn through the data is a fit to a cosine function. To predict the expected peak-to-peak modulation depth it is necessary to identify the extreme levels of A_n corresponding to 0 and π phase difference across the aperture. Although we never know the exact bias state, we can make a close estimate of the expected modulation, based on a staircase that has the features of a 0 bias case (equal length steps). This method will slightly overestimate the depth of the modulation. The observed depth of the modulation is 1.6×10^{-12} m which, based on the above mentioned procedure, corresponds to a phase difference across the aperture of 0.51π. Based on the computed flow pattern in the device (we use a commercial program to solve Laplace's equation in the channel) we predict that the rotation of the Earth will make a phase difference across the aperture of 0.46π. The small difference between the observed number and predicted value is due to the systematic uncertainties in determining the zero bias staircase and in predicting the flow pattern in the device. Random uncertainty arises from the stochastic nature of the phase slip nucleation mechanism and is understood in the context of a thermal activation model.[7]

We have also observed that the modulation of other points on the staircase follows equation (3). For instance, point P2 in Fig. 2 is found to change as $-\cos\alpha$, which is the expected response.

When the bias is anywhere between approximately $\pi/4$ and $3\pi/4$, the modulation of the first plateau should pass through $\cos\alpha = 0$ when the normal to the toroidal plane is oriented in an east–west direction. We find the median level in the modulation to occur when the toroidal plane normal points within ~5° of true east–west. The uncertainty is systematic and is due to a lack of knowledge of the precise orientation of the silicon wafer within the crysostat.

It is interesting to consider the projected sensitivity of this type of device for terrestrial rotation measurements. The present device has

the sensitivity to detect a change in the Earth's rotation, Ω_E, of ~0.5% in one hour. The peripheral channel could be made with multiple turns and could also be enlarged in scale. For a 30-turn tubular channel, with $R = 3$ cm and channel diameter of 1.6 mm, a one-hour measurement time could resolve a rotation change equal to $5 \times 10^{-6}\,\Omega_E$. To achieve this projected sensitivity, vorticity in the tube must be completely pinned, for instance by filling the tube with a porous medium. It remains to be seen if this superfluid rotation sensor would surpass other techniques such as ring laser gyroscopes, atomic interferometers or spinning balls. □

Received 12 December 1996; accepted 10 March 1997.

1. Gregory, D. D. Observations of low-lying superfluid states in a rectangular annulus. Thesis, Univ. California, San Diego (1972).
2. Guernsey, R. W. in *Proc. 12th Int. Conf. on Low Temperature Physics* 79–81 (Keigaku, Tokyo, 1971).
3. Crooker, B. C. Studies of the flow properties of superfluid ^{3}He and of the superfluid density of ^{4}He films in restricted geometries. Thesis, Cornell Univ. (1984).
4. Anandan, J. The Josephson effect in superfluid helium and general relativeity. *J. Phys. A* **17,** 1367–1380 (1984).
5. Bonaldi, M., Vitale, S. & Cerdonio, M. Rotationally induced dissipation in superfluid helium. *Phys. Rev. B* **42,** 9865–9874 (1990).
6. Avenel, O. & Varoquaux, E. Detection of the Earth rotation with a superfluid double-hole resonator. *Czech. J. Phys. (Suppl. S6)* **48,** 3319–3320 (1996).
7. Packard, R. E. & Vitale, S. Principles of superfluid helium gyroscopes. *Phys. Rev. B* **46,** 3540–3549 (1992).
8. Schwab, K. C. Experiments with superfluid oxcillators: design and microfabrication of a superfluid gyroscope; modulation of a ^{4}He rf SQUID analog by the Earth's rotation. Thesis, Univ. California, Berkeley (1996).
9. Zimmermann, Wm. The flow of superfluid ^{4}He through submicron apertures: phase slip and critical velocities due to quantum vortex motion. *Contemp. Phys.* **37,** 219–234 (1996).
10. Avenel, O. & Varoquaux, E. Josephson Effect and quantum phase slippage in superfluids. *Phys. Rev. Lett.* **60,** 416–419 (1988).
11. Schwab, K., Steinhauer, J. Davis, J. C. & Packard, R. E. Fabrication of a silicon-based superfluid oscillator. *J. Microelectromechan. Syst.* **5,** 180–186 (1996).
12. Amar, A., Lozes, R., Sasaki, Y., Davis, J. C. & Packard, R. E. Fabrication of submicron apertures in thin membranes of silicon nitride. *J. Vac. Sci. Technol. B* **11,** 259–262 (1993).
13. Paik, H. J. Superconducting tunable-diaphragm transducer for sensitive acceleration measurements. *J. Appl. Phys.* **47,** 1168–1178 (1976).

Acknowledgements. We thank A. Amar, J. C. Davis, Yu. Mukharsky and J. Steinhauer for help with earlier versions of this experiment; A. Loshak for help with fabrication of the silicon device; S. Vitale, E. Varoquaux, O. Avenel and S. Backhaus for conversations; and R. Orr for preparing Fig. 1. This work was supported in part by the Air Force Office of Scientific Research, the Office of Naval Research, and the National Science Foundation.

Correspondence and requests for materials should be addressed to R.E.P. (e-mail: packard@garnet.berkeley.edu).

Non-volatile memory device based on mobile protons in SiO_2 thin films

K. Vanheusden*, W. L. Warren*, R. A. B. Devine†, D. M. Fleetwood*, J. R. Schwank*, M. R. Shaneyfelt*, P. S. Winokur* & Z. J. Lemnios‡

* *Sandia National Laboratories, Albuquerque, New Mexico 87185-1349, USA*
† *France Telecom/CNET, BP 98, Meylan Cedex, France*
‡ *Defense Advanced Research Projects Agency, Arlington, Virginia 22203-1714, USA*

The silicon/silicon-dioxide system provides the cornerstone of integrated-circuit technology[1]. Since the introduction of devices based on this system, the (largely deleterious) effects on device operation of mobile and trapped charges in the oxide layer have been studied in great detail. Contamination by alkali ions, for example, was a major concern in the early days of metal-oxide–semiconductor device fabrication[2]. But not all SiO_2 impurities are undesirable: the addition of hydrogen, for example, has the beneficial property of rendering charge traps inactive[1]. Here we show that mobile H^+ ions introduced by annealing into the buried oxide layer of Si/SiO_2/Si structures, rather than being detrimental, can form the basis of a non-volatile memory device. These mobile protons are confined to the oxide layer, and their space-charge distribution can be controlled and rapidly rearranged at room temperature by an applied electric field. Memory devices based on this effect are expected to be competitive with current state-of-the-art Si-based memories, with the additional advantage of simplicity—only a few standard processing steps are required.

A variety of Si/SiO_2/Si materials was investigated. A first group, silicon-on-insulator (SOI) materials, consisted of amorphous SiO_2 buried underneath a single crystalline thin Si film. This group included 'separation by the implantation of oxygen' (SIMOX) material formed by high-energy/high-dose ion implantation of oxygen into a Si wafer, and Unibond, which uses a thermally oxidized wafer and wafer-bonding technology to obtain the SOI structure. Apart from these 'technologically advanced' SOI materials, we also studied a second group of standard thermally grown SiO_2 capped with a poly-Si layer. The common processing treatment for all the above structures was a high-temperature 'formation anneal' (1,100–1,300 °C) in an inert atmosphere (1% O_2 added). It was observed that this anneal step was crucial as a pretreatment for the subsequent incorporation of mobile protons in the buried oxide, probably because it created defects in the buried oxide which may be catalyst sites for the generation of atomic hydrogen[3]. A schematic cross-section of the final structure can be seen in Fig. 1b. The top Si layer thickness was typically 200 nm, while the buried oxide varied between 1 μm and 40 nm.

Small isolated islands (3 mm^2) of top Si layer were created to facilitate lateral diffusion of hydrogen (or deuterium) into the buried oxide during anneal treatments in forming gas (N_2 with 5 vol.% of H_2 or D_2, 99.999% pure) and nitrogen (N_2 99.999% pure). Annealing in forming gas between 500 and 800 °C was found to induce a reversible flat-band voltage shift at the top-Si/SiO_2 interface. Figure 2 shows this reversible shift in the drain-current/gate-voltage I_D–V_G curves measured on a SIMOX substrate. Similar features were observed in other SOI materials and in poly-Si capped thermal oxide substrates. No reversible shift could be observed after annealing in N_2 as opposed to forming gas, showing that the presence of hydrogen in the anneal atmosphere is crucial. A detailed

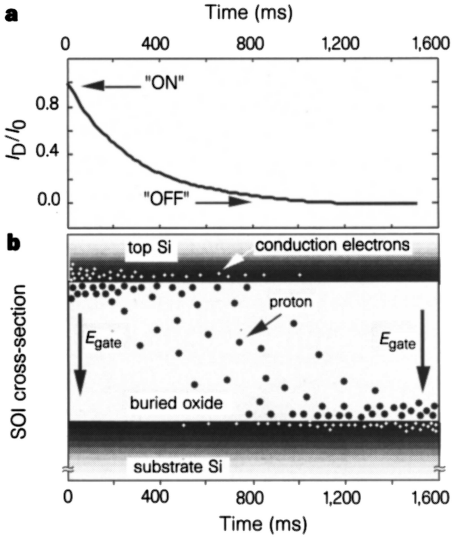

Figure 1 a, Normalized decay of drain current (I_D) versus time at room temperature in a point-contact device with a 40-nm layer of buried silicon oxide, annealed in forming gas at 600 °C. The positive ions were first drifted to the top-Si/SiO_2 interface under positive gate bias (V_G) followed by switching to $V_G = -2$ V (-0.5 MV cm^{-1}). **b**, Cross-sectional schematic of the evolution of mobile charged species in the device on the same timescale, visualizing the applied electric field (E_{gate}) induced drift of the H^+ ions in the buried oxide from the top to the bottom interface, and its effect on the conduction electron density in the conduction channels near the interfaces.